Large-Area Vapor-Phase Growth and Characterization of MoS_2 Atomic Layers on a SiO_2 Substrate

Yongjie Zhan, Zheng Liu, Sina Najmaei, Pulickel M. Ajayan, and Jun Lou**

Monolayer molybdenum disulfide (MoS_2),[1] a 2D crystal with a direct bandgap, is a promising candidate for 2D nanoelectronic devices complementing graphene,[2] receiving increasing attention due to their potential for a range of applications.[3] Unlike conductive graphene and insulating hexagonal boron nitride (h-BN),[4] atomic-layered MoS_2 is a semiconductor material with a direct bandgap, offering possibilities of fabricating high-performance devices with low power consumption in a more straightforward manner.[3a] There have been recent attempts to produce MoS_2 layers via chemical and mechanical exfoliation of bulk material. However, the traditional mechanical exfoliation method is still employed to obtain the MoS_2 atomic layer with rather modest foot-print, limiting its usefulness in a commercially viable device. Liquid exfoliation of layered materials including MoS_2 has been proposed to be a promising large-scale synthesis method for a 2D nanosheet.[5] Although it is quite facile to create hybrid dispersions or composites using this method, its application into device applications still needs further development. Other methods, including hydrothermal methods that were employed to synthesize MoS_2 nanosheet, have similar limitations.[6] Therefore, large-area synthesis of mono- and few-layer MoS_2 that is compatible with current micro- or nanofabrication processes will greatly facilitate the integration of this fascinating material into future device applications.[7] Here we demonstrate the large-area growth of MoS_2 atomic layers on SiO_2 substrates by a scalable chemical vapor deposition (CVD) method. The as-prepared samples can either be readily utilized for further device fabrication or be easily released from SiO_2 and transferred to arbitrary substrates. High-resolution transmission electron microscopy (HRTEM) images and Raman spectra of the as-grown MoS_2 indicate that the number of layers range from a single layer to a few layers. Our results on the direct growth of MoS_2 layers on dielectric leading to facile device fabrication possibilities show the expanding set of useful 2D atomic layers, on the heels of graphene, which can be controllably synthesized and manipulated for many applications.

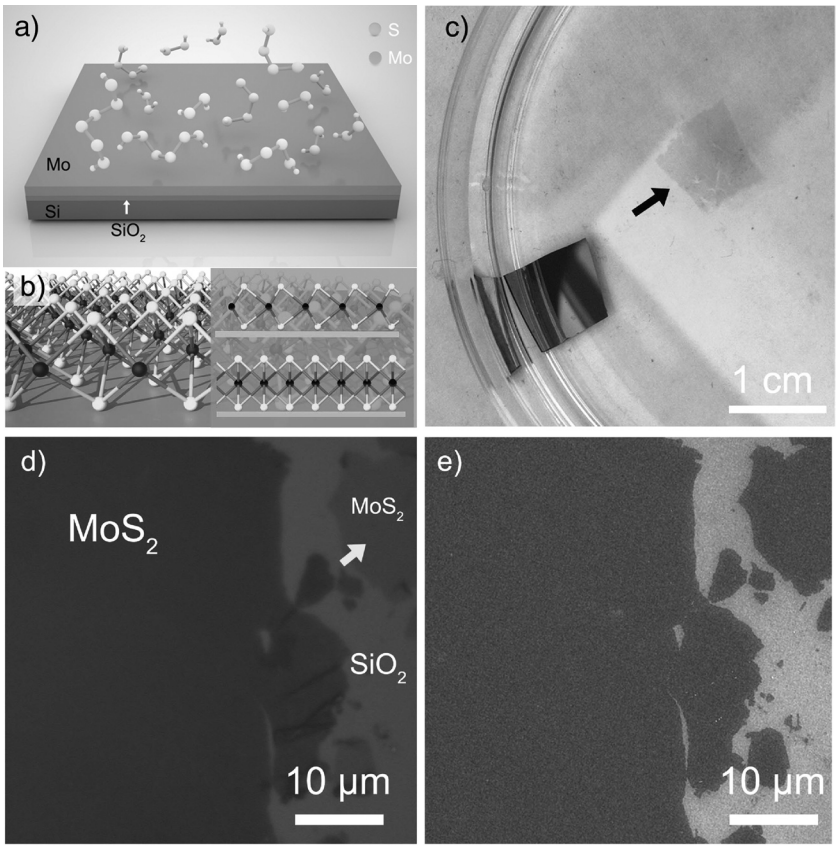

Figure 1. Illustrations and morphologies of atomic-layered MoS_2. a) Introducing sulfur on the Mo thin film that was pre-deposited on the SiO_2 substrate. b) MoS_2 films that are directly grown on the SiO_2 substrate. The atoms in black and yellow represent Mo and S, respectively. c) SiO_2 substrate (left) and peeled-off few-layered MoS_2 (right, indicated by the arrow). d) Optical image of one local section with MoS_2 on the SiO_2 substrate. Most of areas in dark grey are few-layered MoS_2. The area in light grey is (1–2)-layered MoS_2 marked by an arrow. e) Corresponding SEM image. These images show a large size, uniform, and continuous MoS_2 atomic layer.

Dr. Y. Zhan,[+] Dr. Z. Liu,[+] S. Najmaei,
Prof. P. M. Ajayan, Prof. J. Lou
Department of Mechanical Engineering
& Materials Science
Rice University
Houston, Texas 77005, USA
E-mail: ajayan@rice.edu; jlou@rice.edu
[+] These authors contributed equally to this work.

DOI: 10.1002/smll.201102654

small NANO MICRO

As illustrated in **Figure 1**a, a thin layer of Mo (typical thickness ~1–5 nm) was pre-deposited on SiO_2 by an e-beam evaporator at a rate of ~0.1 Å/s. Sulfur is introduced and reacted with Mo at 750 °C forming very thin MoS_2 film (form single layer to few layers), as illustrated in Figure 1b. The as-prepared MoS_2 atomic layers on SiO_2 substrates are readily available for further characterizations as well as device fabrications. It is also easy to transfer the thin layers onto arbitrary substrates by etching away the SiO_2. Figure 1c shows a floating CVD-MoS_2 film (~0.8 cm × 0.8 cm) after it was releasd from SiO_2. The lateral size of the MoS_2 layers is simply dependent on the size of the substrates used, suggesting that the process is scalable, and films of any size can be grown with good uniformity. The thickness of the MoS_2 grown directly relates to the thickness of the pre-deposited Mo metal on the substrate and hence the thickness of the layers can be controlled. The MoS_2 atomic layers can then be transferred onto arbitrary substrates for further characterizations and processing. Figure 1d shows an optical image captured from the edge of a typical MoS_2 on a SiO_2 substrate (285 nm). The light grey area in the top-right corner marked by the while arrow shows a very thin area (1–2 layers), while most of other areas are few-layered MoS_2 in dark grey. Figure 1e shows the corresponding scanning electron microscopy (SEM) image. The morphologies reveal that the on-site growth of MoS_2 on SiO_2 substrate can produce very thin, continuous, and uniform atomic layers. More optical and SEM images can be found in the Supporting Information (SI), Figure S1. In our experiments, we tried to deposite Mo on various substrates (Si, SiO_2, Al_2O_3, Cr, Au, Au/Cr bi-layer) using e-beam evaporation. All other substrates (Al_2O_3, Cr, Au, and Au/Cr) were pre-deposited thin films on silicon wafers. The growth of MoS_2 on different substrates is compared in the SI, Figure S2 and S3.

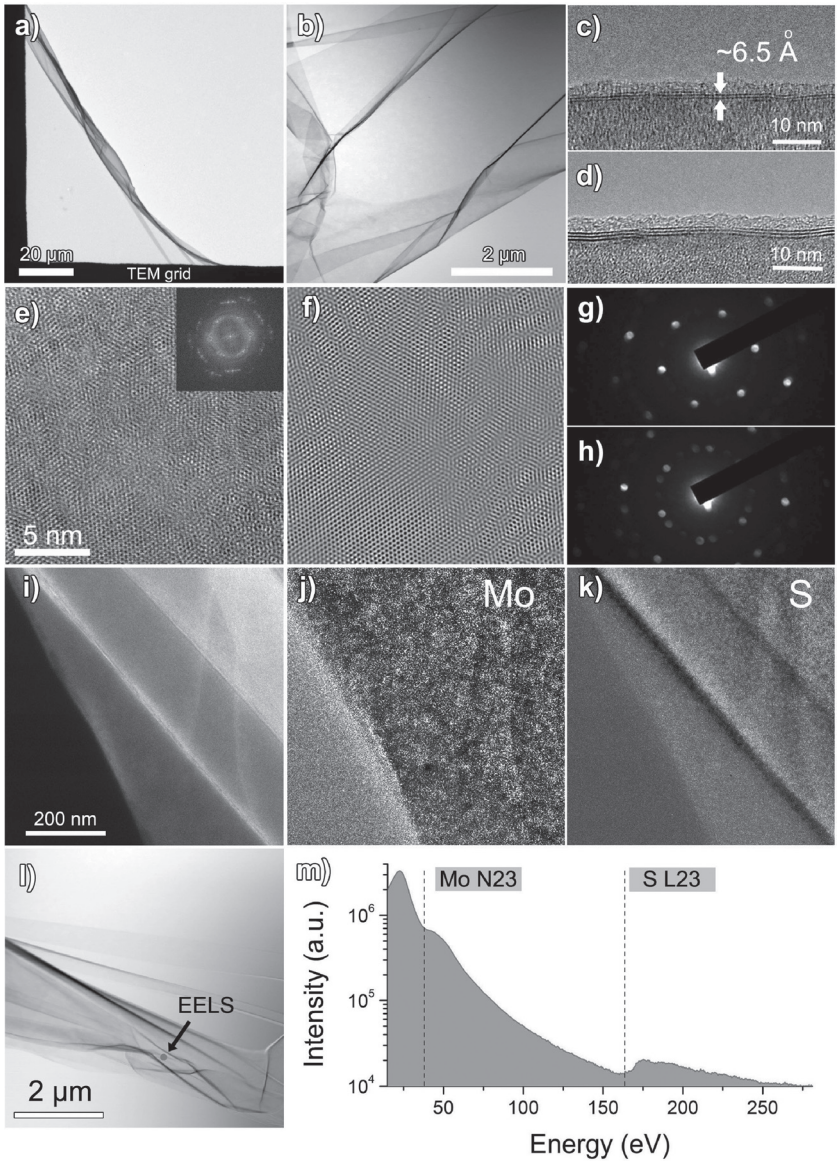

Figure 2. TEM characterizations and chemical elemental analysis of CVD-MoS_2. a) One atomic MoS_2 layer covers the TEM grid. b) Edge area of the atomic MoS_2 layer in (a). c,d) Two and three layers of MoS_2. The distance between two layers is about 6.5 Å. e) A HRTEM image with Moiré patterns. The FFT in the inset reveals a three-layer packing. f) Atomic layers reconstructed by masking the FFT pattern from (e). g,h), Diffraction patterns of the atomic layers. i–k) Original image and corresponding molybdenum and sulfur elemental mappings, indicating the uniform distribution of Mo and S elements. l,m) EELS shows the Mo edge and S edge at ~35 and ~165 eV, respectively. The arrow indicates the area where EELS data was collected.

To further confirm the quality of the MoS_2 atomic layers prepared by our CVD method, **Figure 2**a shows the morphology of an atomic MoS_2 layer covering on the bottom left region of the TEM grid with a rolled-up edge, and Figure 2b shows the close-up of the edge area. Figure 2c,d show two- and three-layered MoS_2 samples. The interlayer spacing is measured to be ~6.6 ± 0.2 Å. The thickness is also confirmed by the atomic force microscopy (AFM) image (SI, Figure S4). Figure 2e is a HRTEM image of a random area of CVD-MoS_2 with Moiré patterns. Figure 2f is atomic layers of MoS_2 reconstructed by masking the fast Fourier transform (FFT) patterns in the inset of Figure 2e. More images are shown in the SI, Figure S5. Figure 2g,h are diffraction patterns of random regions. Figure 2i–k show elemental mappings. Figure 2i is the original image, and Figure 2j and 2k are Mo and S elemental mappings, respectively. The electron energy loss spectrosopy (EELS) results are also shown in Figure 2l,m. The EELS spectrum obtained from the location, indicated by the arrow in Figure 2l, reveals the characteristic peaks of Mo at 35 eV (N-edge) and S at 165 eV (L-edge).[8] The ratio of Mo and S

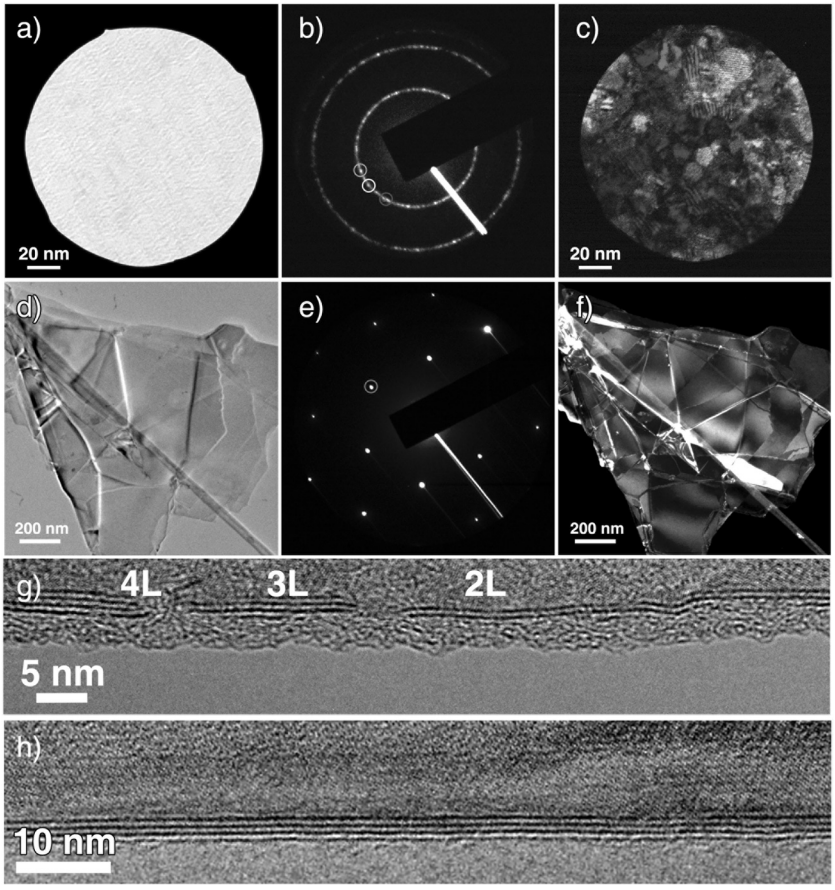

Figure 3. Comparison of grain size in CVD-MoS_2 and LE-MoS_2. a) Random area of CVD-MoS_2 appear uniform in BF-TEM images. b) Diffraction pattern taken from of area in a show the MoS_2 is polycrystalline. c) DF-TEM image corresponding to a false color. d) BF-TEM image of a LE-MoS_2 flake. e) Diffraction pattern taken from a region in d showing a single-crystal MoS_2. f) A corresponding DF-TEM image. g,h) Typical edges of CVD-MoS_2 and LE-MoS_2.

is about 1:2, which is confirmed by the X-ray photoelectron spectroscopy (XPS) data (SI, Figure S6).

The grain size of CVD-MoS_2 and liquid exfoliated MoS_2 (LE-MoS_2),[5] as a comparison, could be estimated by the dark-field (DF) TEM images shown in **Figure 3**. Figure 3a shows a bright-field (BF) TEM image of a random area in the CVD-MoS_2. Figure 3b,c are corresponding diffraction pattern and false-color DF-TEM image of area in Figure 3a, suggesting a polycrystalline MoS_2 with a grain size ranging from 10 to 30 nm. Figure 3b contains multigroup sixfold-symmetry spots, which are also seen in CVD-graphene.[9] The false-color DF-TEM image is taken using an objective aperture filter to cover three spots in the back focus plane, marked by the circle. The greyscale in the DF-TEM image correspond to the ones of circles in Figure 3b. Figure 3d, e, and f are the BF-TEM image, diffraction pattern, and DF-TEM image of LE-MoS_2, respectively. The individual sixfold-symmetry pattern and DF-TEM image suggests the grain size is larger than 1 μm. We also examine the edges in CVD and LE-MoS_2, as shown in Figure 3g,h. The following few-layered samples were observed: four- (4L) and three-layered (3L) at a length of ~10 nm, double-layered (2L) MoS_2 at a length of ~20 nm in CVD-MoS_2, and 4L at a length of ~90 nm in LE MoS_2. These results are future confirmed by the X-ray diffraction (XRD) analysis (SI, Figure S7).

Raman spectra on few-layered as-prepared CVD-MoS_2 and mechanically exfoliated MoS_2 (ME-MoS_2) flakes were collected for comparisons. As shown in **Figure 4**, Raman spectra were collected for single- and double-layered MoS_2 samples on SiO_2 substrate. Two typical Raman active modes could be found: E^1_{2g} at 383 cm^{-1} and A_{1g} at 409 cm^{-1}.[10] These modes of vibration have been investigated both theoretically and empirically in bulk MoS_2;[11] E^1_{2g} indicates planar vibration and A_{1g} is associated with the vibration of sulfides in the out-of-plane direction as illustrated in the inset of Figure 4a. Some criterion could be used to roughly identify the thickness of the layers:[10] 1) Raman peak location and intensity of E^1_{2g} and A_{1g} (with same parameters such as laser power and collecting time). The peaks were found to be blue-shifted for E^1_{2g} and red-shifted for A_{1g} when the film became thinner, which would also result in a weaker signal. In Figure 4a and b, their peaks from E^1_{2g} and A_{1g} located at (384.6 and 405.1 cm^{-1}) and (384.6 and 406.9 cm^{-1}), respectively, which corresponded to single- and double-layered MoS_2 samples. The spectra in blue are recorded from ME-MoS_2 with a corresponding number of layers.[10] 2) the peak spacing between E^1_{2g} and A_{1g}. In our case, they were 20.6 cm^{-1} for single-layered and 22.3 cm^{-1} for double-layered samples; 3) The intensity ratio between the characteristic peaks from MoS_2 and the substrate. For our samples, E^1_{2g}/Si were ~0.05 and 0.09, again corresponding to single- and double-layered MoS_2 samples.[10] The Raman intensity ratios for E^1_{2g} and A^1_g are different for the CVD-MoS_2 and ME-MoS_2. This is because the planar vibration (E^1_{2g}) is subject to the nanoscale and randomly distributed grains in CVD-MoS_2 (Figure 3c), therefore showing a lower relative intensity compared to ME-MoS_2. This is supported by further studies on the DF-TEM image of LE-MoS_2 flakes. Their grain size is much larger, typically on the order of micrometers or more (Figure 3f). Raman mapping was taken from the dashed area (35 μm × 45 μm) shown in Figure 4c, which is a typical edge area of a large-size CVD-MoS_2. Figure 4d and e represent the intensity mapping (E^1_{2g}) and intensity ratio mapping (E^1_{2g}/Si), respectively. There are a total of 576 (24 × 29) Raman spectra collected from this area. Both mappings show a similar landscape. Intensity ratio mapping provides a more accurate characterization and better resolution for the atomic layer samples with different thicknesses. The thin area is shown in dark grey and thick area in light grey. Raman spectra strongly suggest good quality, uniform coverage of MoS_2 atomic layers (from a single layer to a few layers) on the SiO_2 substrate.

Field-effect transistor (FET) devices[7,12] were made by a photolithography process to study the electric transport

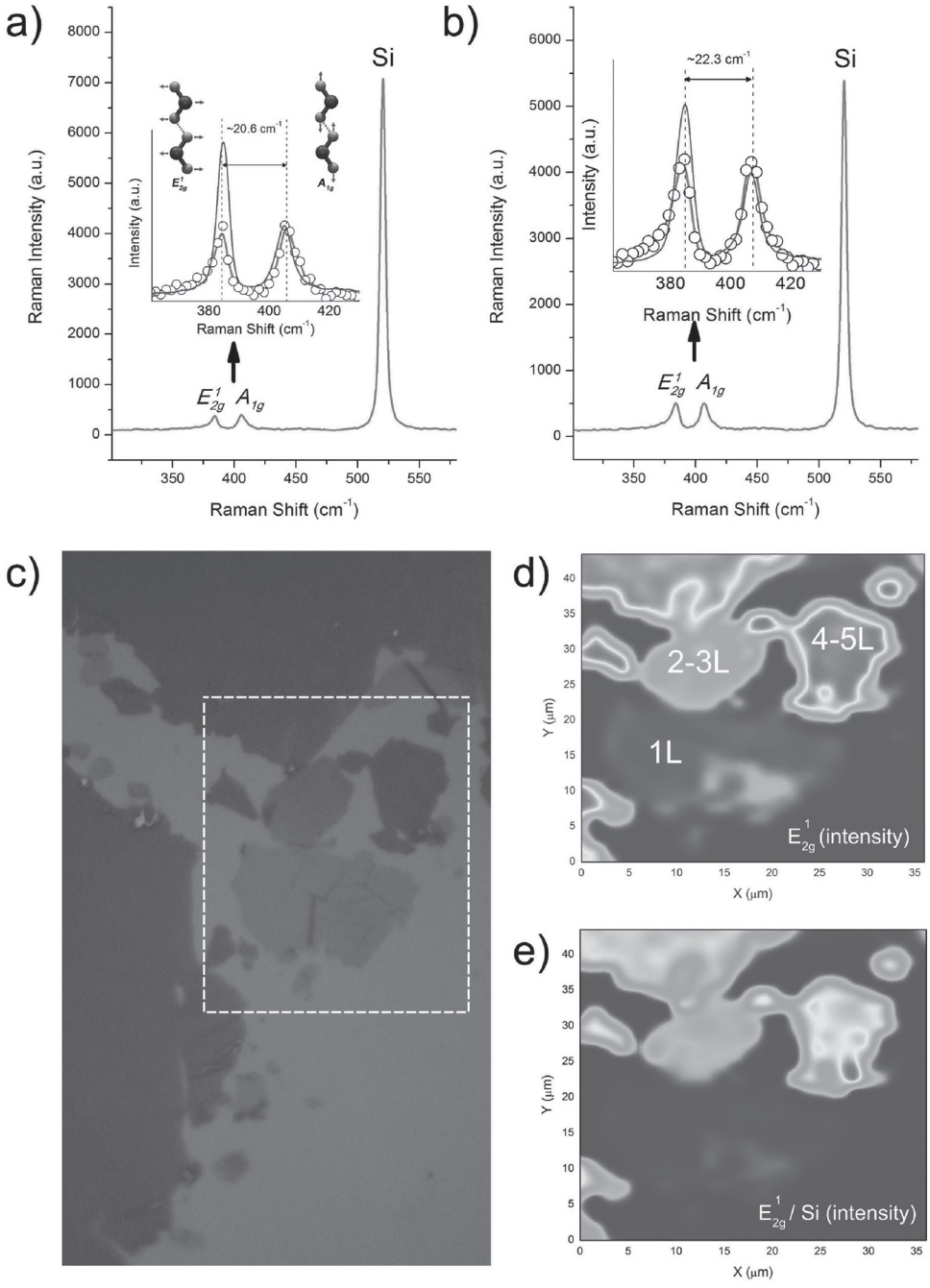

Figure 4. Raman signatures of as-prepared CVD-MoS_2. a,b), Raman spectra of single- and double-layered MoS_2. The thickness of MoS_2 layers can be estimated by evaluating their relative intensity to Si, or the spacing between two vibrating modes (E^1_{2g} and A_{1g}), as shown in the inset. Spectra in solid line in the insets are from ME-MoS_2 (single-layered MoS_2 (a) and double-layered (b)). c) A typical landscape of MoS_2 atomic layers on SiO_2 substrate. The dotted area is mapped in (d) as the intensity of the E^1_{2g} peak, and in (e), as the intensity ratio E^1_{2g}/Si, indicating the number of layers.

properties of CVD-MoS_2. We coated photoresists, LOR5B or S1813, on the CVD-MoS_2, to make electrodes patterns. They were then exposed using a mask aligner (SUSS Mask Aligner MJB4) and developed with MF319 to form undercut structures. Ti/Au electrodes (5 nm/30 nm) were deposited by an e-beam evaporator. The evaporating rate was well controlled about 1 Å/s for Ti and 10 Å/s for Au. The photoresists could be removed using acetone and REMOVER PG (MicroChem). The electrical measurements were carried out using two Keithley 2400 source meters connected with a CTI Cryodyne Refrigeration System to provide a temperature range of 15–450 K and vacuum down to 7×10^{-6} Torr. Their electrical transport properties are shown in **Figure 5**. Figure 5a shows a typical device with an electrode spacing of ~9 μm, and the length of the electrodes is ~100 μm. Figure 5b is a typical current–voltage (I–V) curve of a MoS_2 device with a resistance of ~130 kΩ. For most of the devices, their source current versus bias voltage is linear ranging from

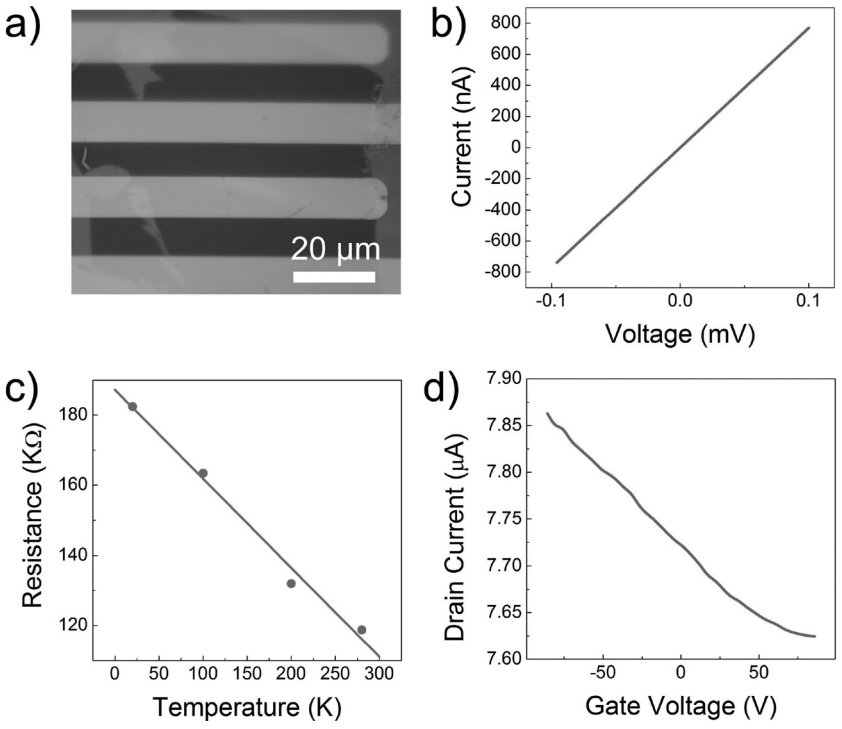

Figure 5. Characterizations of CVD-MoS_2 devices. a) Optical image of a typical MoS_2 device. b) I_{ds}– V_{ds} curve acquired without a gate voltage. c) Temperature dependence of the resistance from 300 to 20K. d) Plot of gate voltage versus drain current.

1 mV to 1 V, suggesting ohmic contacts with our Ti/Au electrodes. The resistivity of our CVD-MoS_2 samples are from ~1.46 × 10^4 to 2.84 × 10^4 Ω/□, about two orders of magnitude higher than CVD-graphene (125 Ω/□).[13] Temperature dependence measurements indicate that the resistance of MoS_2 increases at low temperatures, as shown in Figure 5c. The typical mobilities measured are ranging from 0.004 to 0.04 $cm^2 V^{-1} s^{-1}$ at room temperature, one to two orders of magnitude less than the ME-MoS_2 samples (~0.1–10 $cm^2 V^{-1} s^{-1}$).[14] The mobility of MoS_2 at low field effect is estimated using $\mu = [dI_{ds}/dV_{bg}] \times [(L/(WC_iV_{ds})]$. Here L is the channel length (~9 μm), and W is the channel width (from 17 to 80 μm for various devices). I_{ds}, V_{bg}, and V_{ds} are the source–drain current, the back-gate potential, and the source–drain potential, respectively. C_i (~1.3 × 10^{-4} F m^{-2}) is the capacitance between the channel and the back-gate per unit area. We believe that the low mobilities originate from the planar defect—the nanoscale and randomly distributed CVD-MoS_2 grains, as shown in the DF-TEM image in Figure 3c. In addition, other defects including cationic vacancies, dislocation, and the adsorption-induced doping effect in the MoS_2 are also possible reasons for the low mobilities, which are always observed in CVD-prepared 2D materials such as graphene.[9] The mobility could be significantly improved by annealing the as-prepared samples,[3a,15] using a local top-gate with a high κ dielectric,[3a,16] and optimizing the growth conditions.

The reaction mechanism for synthesizing MoS_2 could be simply understood as a direct elemental chemical reaction. In our experiments, the earlier reported precursors used in synthesizing MoS_2 nanostructures[17] were not selected, since it is very difficult to obtain large-area uniform films from those precursors. Metal substrates have also been considered in experiments. In fact, the reactions between S and metals at relevant reaction temperatures make Au almost the only suitable metal substrate. The resulting MoS_2 grown on such substrate display many interesting tentlike microstructures (SI, Figure S8 and S9). These suspended, perhaps pre-stressed, atomic layers could have some unique properties and also help us learn more about the mechanical properties of such MoS_2 samples.

In summary, we have shown here a direct preparation of single- and few-layered MoS_2 on SiO_2 substrates using a pre-deposition of Mo film followed by CVD method. The size and thickness of the atomic MoS_2 layer only depend on the size of the substrate and the thickness of the pre-deposited Mo, which are easily scalable and controllable, making it possible to meet the demands from different applications. Characterization such as HRTEM images and Raman spectra indicate the CVD-MoS_2 ranges typically from a single layer to a few layers. Our new large-area synthesis method has thus revealed the new possibility of preparing large-area good-quality MoS_2 atomic layer materials, increasing the number of possible candidates to be engineered into 2D structures in the direction provided by the advent of graphene and its applications.

Experimental Section

In a typical procedure, samples (Mo thin films deposited on SiO_2 substrates) placed in a ceramic boat were placed in the center of a tube furnace (Lindberg, Blue M, quartz tube). Another ceramic boat holding pure sulfur (1–2 g, Fisher Scientific, USP grade) was placed in the upwind low-temperature zone in the quartz tube. During the reaction, the temperature in the low-temperature zone were controlled to be a little above the melting point of sulfur (113 °C). The quartz tube was first kept in a flowing protective atmosphere of high-purity N_2, the flow rate of which was set at 150–200 sccm. After 15 min of N_2 purging, the furnace temperature was gradually increased from room temperature to 500 °C in 30 min. Then the temperature was increased again from 500 to 750 °C in 90 min and was kept at 750 °C for 10 min before being cooled down to room temperature in 120 min. Figure S1 in the SI shows a schematic illustration of the reaction condition of this CVD process.

Raman spectroscopy (Renishaw inVia) was performed with a 514.5 nm laser excitation. The scanning electron microscope (FEI Quanta 400) and high-resolution transmission electron microscopy (HRTEM, JEOL-2100) equipped with EELS and GIF filters were employed for imaging and chemical analysis of the samples. XPS (PHI Quantera) was performed using monochromatic aluminum KR X-rays. MultiPak software was used for XPS data analyses. XRD

NANO MICRO small

(Rigaku D/Max Ultima II) was performed using Cu Ka radiation, graphite monoichrometer and scintillation counter.

Supporting Information

Supporting Information is available from the Wiley Online Library or from the author.

Acknowledgements

J.L., Y.Z., Z.L., and S.N. acknowledge the support by the Welch Foundation grant C-1716, the Air Force Research Laboratory grant AFRL FA8650-07-2-5061, and the NSF grant CMMI 0928297. P.M.A. and Z.L. acknowledge funding support from the Office of Naval Research (ONR) through the MURI program on graphene. P.M.A and S.N. acknowledge funding from the Army Research Office through MURI program on Novel Free-Standing 2D Crystalline Materials focusing on Atomic Layers of Nitrides, Oxides, and Sulfides. The authors would like to acknowledge Miss Wei Gao for her help on XRD tests, Mr. Yusuke Nakamura for his help on CVD growth, and Mr. Jiangnan Zhang for his help on measuring Mo film thickness.

[1] a) H. Hadouda, J. Pouzet, J. C. Bernede, A. Barreau, *Mater. Chem. Phys.* **1995**, *42*, 291; b) H. S. S. Ramakrishna Matte, A. Gomathi, A. K. Manna, D. J. Late, R. Datta, S. K. Pati, C. N. R. Rao, *Angew. Chem.* **2010**, *49*, 4153; *Angew. Chem., Int. Ed.* **2010**, *49*, 4059; c) A. Albu-Yaron, M. Levy, R. Tenne, R. Popovitz-Biro, M. Weidenbach, M. Bar-Sadan, L. Houben, A. N. Enyashin, G. Seifert, D. Feuermann, E. A. Katz, J. M. Gordon, *Angew. Chem.* **2011**, *123*, 1850; *Angew. Chem., Int. Ed.* **2011**, *50*, 1810; d) L. P. Hansen, Q. M. Ramasse, C. Kisielowski, M. Brorson, E. Johnson, H. Topsøe, S. Helveg, *Angew. Chem.* **2011**, *123*, 10335; *Angew. Chem., Int. Ed.* **2011**, *50*, 10153.

[2] a) X. Li, W. Cai, J. An, S. Kim, J. Nah, D. Yang, R. Piner, A. Velamakanni, I. Jung, E. Tutuc, S. K. Banerjee, L. Colombo, R. S. Ruoff, *Science* **2009**, *324*, 1312; b) K. S. Novoselov, A. K. Geim, S. V. Morozov, D. Jiang, Y. Zhang, S. V. Dubonos, I. V. Grigorieva, A. A. Firsov, *Science* **2004**, *306*, 666; c) Z. Liu, L. Song, S. Z. Zhao, J. Q. Huang, L. L. Ma, J. N. Zhang, J. Lou, P. M. Ajayan, *Nano Lett.* **2011**, *11*, 2032.

[3] a) B. Radisavljevic, A. Radenovic, J. Brivio, V. Giacometti, A. Kis, *Nat. Nanotechnol.* **2011**, *6*, 147; b) A. Splendiani, L. Sun, Y. Zhang, T. Li, J. Kim, C.-Y. Chim, G. Galli, F. Wang, *Nano Lett.* **2010**, *10*, 1271; c) G. Eda, H. Yamaguchi, D. Voiry, T. Fujita, M. Chen, M. Chhowalla, *Nano Lett.* **2011**.

[4] R. R. Nair, W. Ren, R. Jalil, I. Riaz, V. G. Kravets, L. Britnell, P. Blake, F. Schedin, A. S. Mayorov, S. Yuan, M. I. Katsnelson, H.-M. Cheng, W. Strupinski, L. G. Bulusheva, A. V. Okotrub, I. V. Grigorieva, A. N. Grigorenko, K. S. Novoselov, A. K. Geim, *Small* **2010**, *6*, 2773.

[5] J. N. Coleman, M. Lotya, A. O'Neill, S. D. Bergin, P. J. King, U. Khan, K. Young, A. Gaucher, S. De, R. J. Smith, I. V. Shvets, S. K. Arora, G. Stanton, H. Y. Kim, K. Lee, G. T. Kim, G. S. Duesberg, T. Hallam, J. J. Boland, J. J. Wang, J. F. Donegan, J. C. Grunlan, G. Moriarty, A. Shmeliov, R. J. Nicholls, J. M. Perkins, E. M. Grieveson, K. Theuwissen, D. W. McComb, P. D. Nellist, V. Nicolosi, *Science* **2011**, *331*, 568.

[6] a) W. X. Chen, L. Ma, H. Li, Y. F. Zheng, Z. D. Xu, *Mater. Lett.* **2008**, *62*, *797*; b) Y. T. Qian, Y. Y. Peng, Z. Y. Meng, C. Zhong, J. Lu, W. C. Yu, Y. B. Jia, *Chem. Lett.* **2001**, *772*; c) T. Z. Zou, J. P. Tu, H. D. Huang, D. M. Lai, L. L. Zhang, D. N. He, *Adv Eng Mater* **2006**, *8*, 289.

[7] H. Li, Z. Yin, Q. He, H. Li, X. Huang, G. Lu, D. W. H. Fam, A. I. Y. Tok, Q. Zhang, H. Zhang, *Small* **2012**, *8*, 63.

[8] C. Reza-San Germán, P. Santiago, J. A. Ascencio, U. Pal, M. Pérez-Alvarez, L. Rendón, D. Mendoza, *J. Phys. Chem. B* **2005**, *109*, 17488.

[9] P. Y. Huang, C. S. Ruiz-Vargas, A. M. van der Zande, W. S. Whitney, M. P. Levendorf, J. W. Kevek, S. Garg, J. S. Alden, C. J. Hustedt, Y. Zhu, J. Park, P. L. McEuen, D. A. Muller, *Nature* **2011**, *469*, 389.

[10] C. Lee, H. Yan, L. E. Brus, T. F. Heinz, J. Hone, S. Ryu, *ACS Nano* **2010**, *4*, 2695.

[11] a) S. Jiménez Sandoval, D. Yang, R. F. Frindt, J. C. Irwin, *Phys. Rev. B: Condens. Matter Mater. Phys.* **1991**, *44*, 3955; b) J. L. Verble, T. J. Wieting, *Phys. Rev. Lett.* **1970**, *25*, 362; c) R. A. Bromley, *Philosophical Magazine* **1971**, *23*, 1417.

[12] S. Ghatak, A. N. Pal, A. Ghosh, *ACS Nano* **2011**, *5*, 7707.

[13] S. Bae, H. Kim, Y. Lee, X. Xu, J.-S. Park, Y. Zheng, J. Balakrishnan, T. Lei, H. Ri Kim, Y. I. Song, Y.-J. Kim, K. S. Kim, B. Ozyilmaz, J.-H. Ahn, B. H. Hong, S. Iijima, *Nat. Nanotechnol.* **2010**, *5*, 574.

[14] K. S. Novoselov, D. Jiang, F. Schedin, T. J. Booth, V. V. Khotkevich, S. V. Morozov, A. K. Geim, *Proc. Natl. Acad. Sci. USA* **2005**, *102*, 10451.

[15] A. Ayari, E. Cobas, O. Ogundadegbe, M. S. Fuhrer, *J. Appl. Phys.* **2007**, *101*.

[16] N. J. Tao, F. Chen, J. L. Xia, D. K. Ferry, *Nano Lett.* **2009**, *9*, 2571.

[17] a) A. M. Maja Remskar, Marko Virsek, Matjaz Godec, Matthias Krause, Andreas Kolitsch, Amol Singh, A. Seabaugh, *Nanoscale Res. Lett.* **2011**, *6*, 26; b) X. L. Li, Y. D. Li, *Chem. Eur. J.* **2003**, *9*, 2726; c) F. L. Deepak, A. Mayoral, M. J. Yacaman, *Mater. Chem. Phys.* **2009**, *118*, 392; d) H. A. Therese, N. Zink, U. Kolb, W. Tremel, *Solid State Sci.* **2006**, *8*, 1133; e) F. Deepak, A. Mayoral, M. Yacaman, *Appl. Phys. A: Mater. Sci. Process.* **2009**, *96*, 861; f) M. Viršek, M. Krause, A. Kolitsch, A. Mrzel, I. Iskra, S. o. D. škapin, M. Remškar, *J. Phys. Chem. C* **2010**, *114*, 6458.

[18] N. H. Turner, A. M. Single, *Surf. Interface Anal.* **1990**, *15*, 215.

[19] a) X.-R. Yu, F. Liu, Z.-Y. Wang, Y. Chen, *J. Electron Spec. Relat. Phenom.* **1990**, *50*, 159; b) J. R. Lince, D. J. Carre, P. D. Fleischauer, *Langmuir* **1986**, *2*, 805.

[20] a) I. Alstrup, I. Chorkendorff, R. Candia, B. S. Clausen, H. Topsøe, *J. Catal.* **1982**, *77*, 397; b) G. Seifert, J. Finster, H. Müller, *Chem. Phys. Lett.* **1980**, *75*, 373.

Received: December 16, 2011
Published online: February 15, 2012

